

An Experimental Study of the Line Shape of Orbital Mediated Tunneling Bands Seen in Inelastic Electron Tunneling Spectroscopy

K. W. Hipps* and Ursula Mazur

Department of Chemistry and Materials Science Program, Washington State University, Pullman, Washington 99164-4630

Received: December 17, 1999; In Final Form: February 21, 2000

The line shape of inelastic transitions seen in inelastic electron tunneling spectroscopy (IETS) performed on metal–insulator–adsorbate–metal junctions is well understood. Recently, there have been reports of quasi-elastic processes leading to strong wide bands in what heretofore had been called IETS. It is demonstrated that these quasi-elastic ionizations, known as orbital mediated tunneling (OMT) bands, are actually differential in nature. However, because of the steeply rising elastic background in IETS, and because of the asymmetric shape of these bands, they often give the appearance of simple peaks. It is experimentally shown that the position and width of these false peaks can be used to reasonably estimate the actual maximum in the density of states associated with the orbital mediated transition.

Introduction

Inelastic electron tunneling spectroscopy is an all electron spectroscopy that has been extensively reviewed.^{1–7} By measuring currents and voltages across a metal–insulator–adsorbate–metal (M–I–A–M') device, one is able to extract vibrational and electronic spectroscopic information about the metals, the insulator, and the adsorbate.

In its simplest form, an IET spectrum is a plot of d^2I/dV^2 versus V . It turns out that using $|d^2I/dV^2/(dI/dV)|$ [or $|(d\sigma/dV)/\sigma|$] as the y axis provides spectra having flatter baselines and is most appropriate for high bias work.^{8–11} These are called normalized tunneling intensities (NTI) or constant modulation spectroscopy intensities. Simple tunneling spectra are measured by applying a variable bias, V , and a small modulation component, V_f , at frequency, f . A lock-in amplifier is used to detect the $2f$ signal that is proportional to d^2I/dV^2 . The instrumentation required for obtaining normalized intensities, NTI, is a bit more complex.^{8–10} In general, the bias voltage may be converted to the more conventional wavenumbers through the factor of $8066 \text{ cm}^{-1}/V$. The amplitude of the modulation determines the observed signal strength and resolution, with the signal increasing as V_f^2 while the line width is proportional to V_f .^{1,12}

Until relatively recently, it was assumed that all the bands seen by this method were due to inelastic interactions between the tunneling electron and the barrier region.^{1,13} Kirtley and Soven first considered the possibility of resonant scattering.¹³ They argued that resonant scattering should be signaled by multiple overtones in the coupling vibrations. Since even single overtone bands are almost never seen in IETS,⁶ they concluded that the role of resonant scattering was generally negligible. In the tunnel junction spectroscopy community, this idea was so strongly imbedded that the name, inelastic electron tunneling spectroscopy (IETS), became synonymous with all d^2I/dV^2 vs V spectra. Although it did not receive much attention, a theoretical analysis presented by Persson and co-workers, showed that under certain conditions resonance tunneling via adsorbate electronic states might not produce multiple phonon bands.^{14,16} These conditions, for a single active mode, are that

the vibrational frequency and electronic-vibrational coupling parameter both be small compared to the width of the resonant electronic transition. As the number of active modes increases, the distortion per mode usually grows smaller, thereby reducing the coupling parameter for each mode. Thus, in the case of a complex molecular electronic transition, one might not observe multiphonon transitions.

While resonance-like effects were first attributed to features in the IETS in 1991,¹⁷ the first clear-cut evidence of elastic tunneling via adsorbate molecular orbitals in M–I–A–M' diodes was provided in 1994.^{18,19} Later, Mazur and Hipps proposed a simple model based on electrochemical redox potentials for predicting the position of these bands that they called orbital mediated tunneling (OMT) bands.²⁰ Since then, there has been progress in identifying features in the tunneling spectrum that are associated with quasi-resonant tunneling through adsorbate orbitals, both occupied and unoccupied.^{21,22}

In the STM realm, elastic tunneling via surface states has been well-known and discussed.^{23–25} In this case peaks are observed in dI/dV (or σ) versus bias voltage curves. In the case of semiconductors and metals, these surface state variations are in the electrodes, but cases of adsorbate orbital mediated tunneling in STM are known both in UHV^{22,25} and in solution.^{26–28} In UHV the orbital mediation may take the role of a direct resonance interaction (virtual state) or may be through a phonon-mediated resonance interaction or through simple hopping. In solution STM work, redox enhanced tunneling was predicted on theoretical grounds by Schmickler²⁹ for true resonance processes, and by Kuznetsov³⁰ in the case where there is relaxation of the intermediate ion before the electron is transferred to the opposite electrode. Experimentally, both mechanisms lead to Gaussian-like bands in dI/dV .²⁷ This issue of resonant tunneling versus electron hopping with the molecular ion being an intermediate state is still not resolved. It is presumed that all of these processes would fall under the general topic of orbital mediated tunneling spectroscopy (OMTS). Because of the confusion associated with which mechanism applies to a given process, we in general identify all OMT transitions as associated with quasi-resonance processes.

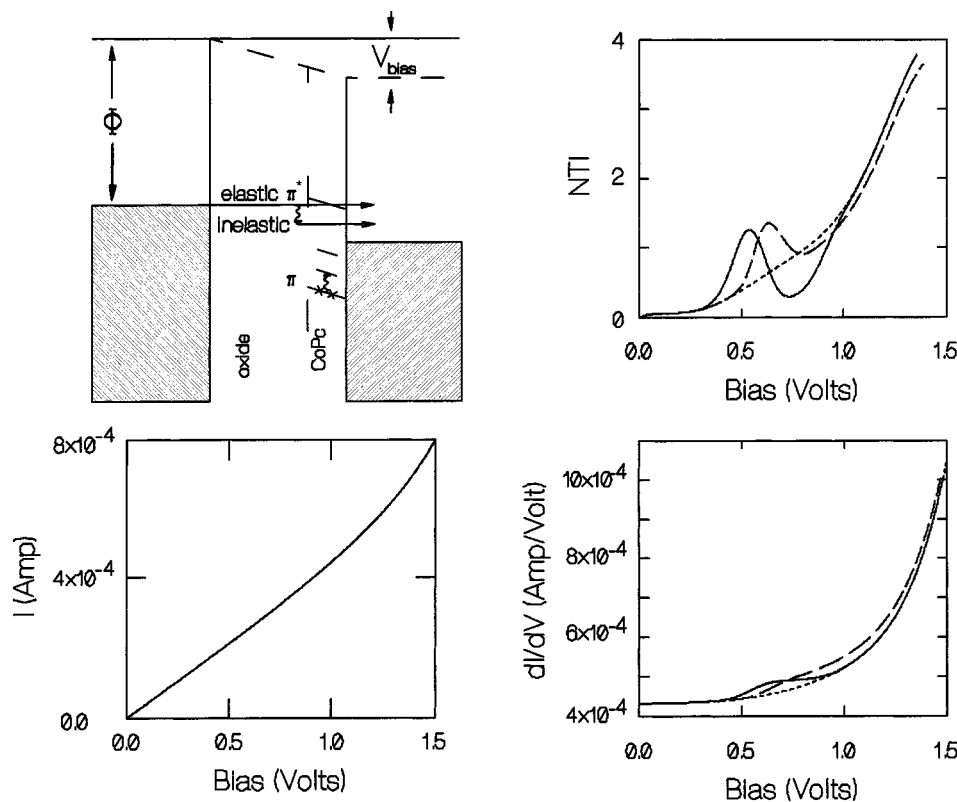


Figure 1. Elastic and inelastic tunneling processes and of the resulting I - V , dI/dV - V , and NTI - V curves in positive bias (right-hand metal biased positively as shown in figure). Dotted curves (···) are for junctions having no OMT or IETS bands, solid curves are for junctions having an OMT band, and broken curves (---) represent data from junctions having a strong inelastic transition.

The purpose of this paper is to address the issue of line shape and peak position of OMT bands in NTI versus V plots, loosely (and incorrectly) identified as IETS. We will demonstrate that past assignments of the position of OMT transitions have a small systematic error and put forth a simple procedure for correcting these values.

Experimental Section

$Al-Al_2O_3-CoPc-Pb$ tunnel diodes were fabricated by the same methods as were employed for other OMTS studies.²¹ The cobalt phthalocyanine (CoPc) was sublimed before use and was deposited to an average thickness of 0.4 nm as determined by a quartz crystal microbalance. Tunneling spectra were collected as normalized tunneling intensities (NTI), which are equivalent to $|(d\sigma/dV)/\sigma|$.^{8,10} The $Al-Al_2O_3-ensil-Pb$ junction was prepared by solution phase doping of *N*-2-aminoethyl-3-amino-propyltrimethoxysilane (ensil), 0.12% in benzene solution.³¹ The NTI spectra of both compounds were measured at 4 K and at 77 K by immersion in liquid helium or liquid nitrogen, respectively. A modulation voltage of 8 mV rms was used and all spectra are the sum of more than 30 scans.

Conductance curves of $Al-Al_2O_3-CoPc-Pb$ tunnel diodes were measured using a configuration similar to that previously described for d^2V/dI^2 spectra,³² but monitoring the lock-in signal at the fundamental frequency rather than the second harmonic. These dV/dI values were then transformed to conductance through the relationship, $\sigma = 1/(dV/dI)$. As in the case of NTI spectra, a modulation voltage of 8 mV rms was used and the diode was held at 77 K. Not presented but recorded were dV/dI curves at various modulation voltages from 0.5 to 50 mV. No significant changes in the results were observed.

Results and Discussion

An energy level diagram for the $[Al-Al_2O_3-CoPc-Pb]$ tunnel junction is shown schematically in Figure 1. This figure

can be used to explain features observed in dI/dV - V and in NTI - V curves. Since more of the tunneling current comes from electrons near the Fermi surface, only those are considered in this cartoon of the process. When the bias is low and there is no structured material in the barrier region, electrons can tunnel elastically across the barrier. This elastic current is nearly linear at low bias and becomes very nonlinear at high bias. From past experience with IETS, it is known that both intense inelastic bands and OMTS bands generally are not directly discernible in the I - V curve. If the tunneling electrons interact inelastically with CoPc, they lose the amount of energy necessary to excite the adsorbate (a vibrational mode in Figure 1) and proceed to tunnel out of the barrier. If the initial energy of the electron is insufficient to both excite the inelastic process and retain energy greater than the right-hand metal Fermi energy, the process is forbidden by the Pauli principal. Thus, there is an onset bias for the inelastic channel to contribute to the tunneling current. For a very intense inelastic electronic excitation, this produces a rounded step in the dI/dV - V curve (the broken line in Figure 1). For quasi-resonant tunneling, where the tunneling electron is absorbed and re-emitted by the CoPc layer, we would expect the dI/dV curve to reflect the density of states for the CoPc (empty states in the case of this example). Thus, a discernible peak in the dI/dV - V curve should be seen for quasi-resonant processes involving the π^* orbital with a local maximum occurring near the bias voltage that aligns the Fermi energy of the left electrode and the CoPc π^* orbital (solid line in Figure 1). The dotted line in Figure 1 is the dI/dV - V curve for a junction lacking either intense IETS or OMT bands.

In the NTI , also shown in Figure 1, the effects of the inelastic excitation (broken line) and the quasi-resonant OMT band (solid line) are easily observed relative to the elastic continuum (dotted line) and also relative to each other. Given a knowledge of the elastic background curve, as we have in this synthetic spectrum,

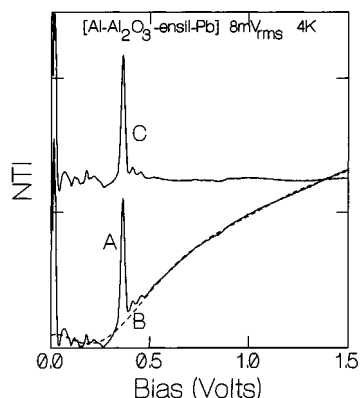


Figure 2. IETS of an Al-Al₂O₃-ensil-Pb junction taken at 4 K and 8 mV modulation. Curve A is the raw data, curve B is a simple polynomial fit to the background, and curve C is the difference between A and B, the background corrected data.

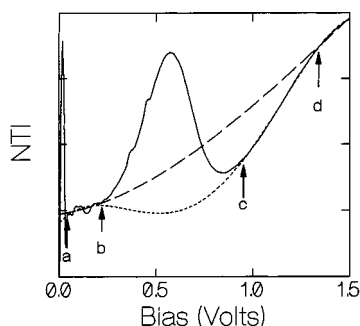


Figure 3. NTI of an [Al-Al₂O₃-CoPc-Pb] tunnel diode taken at 4 K and 8 mV modulation. The solid curve is the raw data. The broken curve is the baseline fit obtained using data in the intervals a-b and d-1.5. The dotted curve is the baseline fit to the data on the intervals a-b and c-1.5.

it is very easy to see that the OMT band is differential in shape while the IETS is a clear peak. Unfortunately, the real world is a bit more complex and finding the correct elastic baseline is often difficult.

Consider the case of a junction having an IETS spectrum composed solely of inelastic vibrational excitations and the elastic continuum. Figure 2A presents the NTI spectrum of such a junction. Note that the elastic background makes it difficult to compare vibrational band intensities and distracts the eye from the vibrational bands. It is now common practice to fit a polynomial to NTI data (excluding intense bands) and to then subtract that background from the data. Both a typical polynomial fit and the resulting difference curve are shown in Figure 2. Because the vibrational bands are sharp, a relatively wide range of background curves produce essentially the same spectral widths and peak positions.

In the case of OMT bands, however, the choice of data range for background fitting makes a significant change in the band shape. Consider, for example, Figure 3, where two (of many) possible choices for regions to be fit are displayed. If one follows the usual IETS procedure and simply omits strong bands from the baseline data for fitting, the dotted curve in Figure 3 is the resulting baseline. If, instead, one anticipates the fact that this band should be differential in nature and uses only high bias data very far from the OMT structure, the broken baseline results. Difference spectra based on these baselines are shown in Figure 4. In the case of the conventional IETS baseline, a single broad band results. Choosing a much wider range of excluded data produces a difference band that is clearly differential in form. Interestingly, *the band maxima are virtually*

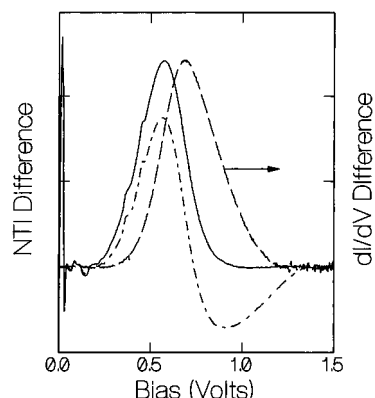


Figure 4. NTI difference spectra from the same junction but with baseline choices made as in Figure 3 and experimental dI/dV difference for the same type of junction. The solid curve is the difference obtained using the dotted baseline in Figure 3. The dash-dot curve is the NTI difference based on the broken curve baseline of Figure 3. The broken curve is the resonant part of the dI/dV curve.

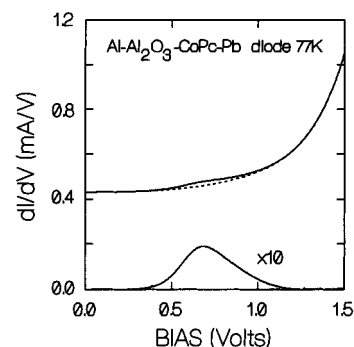


Figure 5. Experimental dI/dV versus V. The dotted curve is the polynomial fit of the elastic continuum background. The lower curve is the difference between the data and the background multiplied by 10.

identical. Thus, while theoretical considerations dictate that the differential shape is the correct one, the band maximum is insensitive to the baseline choice.

Of course, in the case of OMTS bands, the real quantity of interest is the maximum of the dI/dV curve. To better understand how these NTI difference curves relate to the actual band in dI/dV, an experimentally determined dI/dV curve is presented in Figure 5. Also shown in Figure 5 is the density of states for the orbital mediated transition as derived from removing the background generated by the elastic continuum (dotted curve). Note that this band is not symmetrical and tails to high energy, as expected for a system with nonzero vibrational-electronic coupling. That same difference band is also displayed in Figure 4. As expected, the maximum in dI/dV lies above the maxima seen in the NTI; however, the shift is small compared to the width of the bands.

In Figure 4, the band maxima of the NTI difference and the dI/dV band are at 0.573 and 0.686 V, respectively, for a shift of 0.113 V—this is the error introduced by using that apparent maximum in the NTI independent of the background function chosen. The half-width at 1/e height (right side) of the NTI difference band (solid curve in Figure 4) is 0.156 V, and the half-width at half-height is 0.132 V. If, instead, one measures the half-width at half-height for the differential NTI curve (dash-dotted in Figure 4), one finds a value of 0.102 V. Thus, *the error in choosing the maximum in the NTI as the maximum in the density of states associated with the OMT process is approximately the half-width at half-height of the NTI band independent of the baseline chosen.* To see that this should be

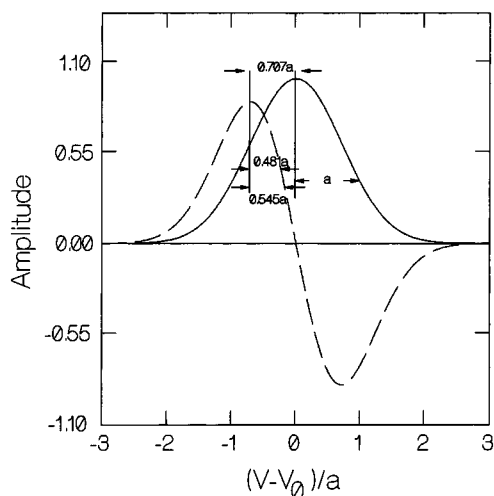


Figure 6. Simple Gaussian and its derivative. If the half-width at the $1/e$ height of the Gaussian is a , the half-width at $1/e$ height on the inner side of the derivative is $0.545a$ and the peak shift is $0.707a$. The half-width at half-height (sharp side) of the derivative is $0.481a$. Thus, the half-width at half-height of the derivative curve represents about 70% of the peak shift.

a fairly general result, consider a simple Gaussian band and a flat baseline, as shown in Figure 6. If a is the half-width at $1/e$ height of the Gaussian, the peak in the derivative is shifted by $0.707a$ and the half-width at half-height of the derivative (on the sharp side) is $0.481a$. Thus, the half-width at half-height of the derivative is $(0.481 \times 100/0.707)$ 68% of the peak shift.

To correct NTI band positions, one must also take into account the bias polarity. For bands in positive bias (those involving unoccupied orbitals), the correction should be added to the peak position. For oxidation bands (those involving occupied orbitals), the correction should be subtracted from the (negative) band maximum. The above observation is important as more than a way of correcting existing NTI data. While it may seem that one should always measure the $dI/dV-V$ curves in order to extract OMTS bands (and we recommend this), this is not always practical. Our ability to extract the band shape from the CoPc dI/dV data relies heavily on the fact that it is the most intense OMT transition we have observed to date. Thus, we could set regions for the baseline fit with reasonable confidence and the noise in the resulting difference spectrum was acceptably low. The high intensity also allowed us to neglect the inelastic contributions to the dI/dV curve. Weaker OMT bands are often not obviously identifiable in the dI/dV curve and the vibrational IETS bands often add to the overall

dI/dV signal. Thus, one runs the risk of significantly changing the OMTS shape with the fitting process required to expose it.

Acknowledgment. K.W.H. thanks Research Corp. for their support in terms of a Research Opportunity Award, and the NSF for their support through grant CHE 9819318. Acknowledgment is also made to the donors of the Petroleum Research Fund, administered by the American Chemical Society, for partial support of this research.

References and Notes

- (1) Hansma, P. K. *Tunneling Spectroscopy*; Plenum Press: New York, 1982.
- (2) Weinberg, W. H. *Vibr. Spectra Struct.* **1982**, *11*, 1.
- (3) Walmsley, D. G.; Tomlin, J. L. *Prog. Surf. Sci.* **1985**, *18*, 247.
- (4) *Vibrational Spectroscopy of Molecules on Surfaces*; Yates, J. T., Madey, T. E., Eds.; Plenum: New York, 1987.
- (5) Reviere, J. C. *Surface Analytical Techniques*; Clarendon: Oxford, U.K., 1990; Chapter 20.
- (6) Hipps, K. W.; Mazur, U. *J. Phys. Chem.* **1993**, *97*, 7803–14.
- (7) Reynolds, S.; Oxley, D. P. *Inelastic electron tunnelling spectroscopy (IETS): principles, applications and future directions*; Future Dir. Thin Film Sci. Technol., Proc. Int. Sch. Condens. Matter Phys., 9th Meeting Date 1996; Marshall, J. M., Ed.; World Scientific: Singapore, 1997; pp 209–217.
- (8) Hipps, K. W.; Mazur, U. *Rev. Sci. Instrum.* **1988**, *59*, 1903–1905.
- (9) Hipps, K. W.; Mazur, U. *J. Phys. Chem.* **1987**, *91*, 5218–5224.
- (10) Seman, T. R.; Mallik, R. R. *Rev. Sci. Instrum.* **1999**, *70*, 2808–2814.
- (11) Hipps, K. W.; Mazur, U. *J. Phys. Chem.* **1987**, *91*, 5218–5224.
- (12) Hipps, K. W.; Peter, S. L. *J. Phys. Chem.* **1989**, *93*, 5717–5721.
- (13) Kirtley, J.; Soven, P. *Phys. Rev.* **1979**, *B19*, 1812.
- (14) Persson, B. N. *J. Phys. Scr.* **1988**, *38*, 282.
- (15) Baratoff, A.; Persson, B. N. *J. Vac. Sci. Technol.* **1988**, *6*, 331.
- (16) Persson, B. N. J.; Baratoff, A. *Phys. Rev. Lett.* **1987**, *59*, 339.
- (17) Hipps, K. W.; Hoagland, J. J. *Langmuir* **1991**, *7*, 2180–2186.
- (18) Mazur, U.; Hipps, K. W. *J. Phys. Chem.* **1994**, *98*, 5824–5829.
- (19) Mazur, U.; Hipps, K. W. *J. Phys. Chem.* **1994**, *98*, 8169–8172.
- (20) Mazur, U.; Hipps, K. W. *J. Phys. Chem.* **1995**, *99*, 6684–6688.
- (21) Mazur, U.; Hipps, K. W. *J. Phys. Chem. B* **1999**, *103*, 9721–9727.
- (22) Hipps, K. W.; Barlow, D. E.; Mazur, U. *J. Phys. Chem. B* **2000**, *104*, 2444–2447.
- (23) Hamers, R. J.; Tromp, R. M.; DeMuth *Phys. Rev. Lett.* **1986**, *56*, 1972.
- (24) Hamers, R. J. *Ann. Rev. Phys. Chem.* **1989**, *40*, 531.
- (25) Hamers, R. J. *J. Phys. Chem.* **1996**, *100*, 13103–13120.
- (26) Tao, N. *J. Phys. Rev. Lett.* **1996**, *76*, 4066–4069.
- (27) Han, W.; Durantini, E. N.; Moore, T. A.; Moore, A. L.; Gust, D.; Rez, P.; Letherman, G.; Seely, G.; Tao, N.; Lindsay, S. M. *J. Phys. Chem. B* **1997**, *101*, 10719–10725.
- (28) Schmickler, W.; Tao, N. *Electrochim. Acta* **1997**, *42*, 2809–2815.
- (29) Schmickler, W. *J. Electroanal. Chem.* **1990**, *296*, 283–289.
- (30) Kuznetsov, A.; Somner-Larse, P.; Ulstrup, J. *Surf. Sci.* **1992**, *275*, 52–64.
- (31) Hipps, K. W.; Mazur, U. *Surf. Sci.* **1989**, *207*, 385–398.
- (32) Hipps, K. W.; Mazur, U. *J. Phys. Chem.* **1980**, *84*, 3162–3172.